UAV trajectory optimization for Precision Agriculture

Cristhian S. Muñoz, Juan S. Corredor, Diego A. Patino, Julian D. Colorado
Department of Electronics Engineering,
Pontificia Universidad Javeriana Bogotá, Colombia, Cr 7 No. 40-62, Bogota, Colombia

***Abstract*—Monitoring large-scale crops using an autonomous UAV demands optimal path planning methods to increase remote sensing autonomy. This paper presents a comprehensive optimization model to minimize the UAV battery consumption during crop monitoring tasks.**

Keywords— UAV, optimization, UAV dynamics and aerodynamics.

I. Introduction

Data acquisition for crop phenotyping requires several types of sensors to measure spatio-temporal variations in crop data. Several applications have adopted the use of Unmanned Aerial Vehicles (UAVs) equipped with multispectral sensors for acquiring aerial imagery at canopy level. This requires UAVs to have greater payload capabilities at the expense of flight autonomy.

In this work, we use an autonomous UAV for the estimation of above-ground biomass in rice crops. We have developed a drone-based solution for capturing multispectral imagery through the entire growth cycle of the crop, as depicted in Fig 1. In turn, the drone requires sufficient flight autonomy to properly sampling the corresponding crop plots. To this purpose, it is essential to extend the autonomy of the aerial vehicle by the means of optimization methods.

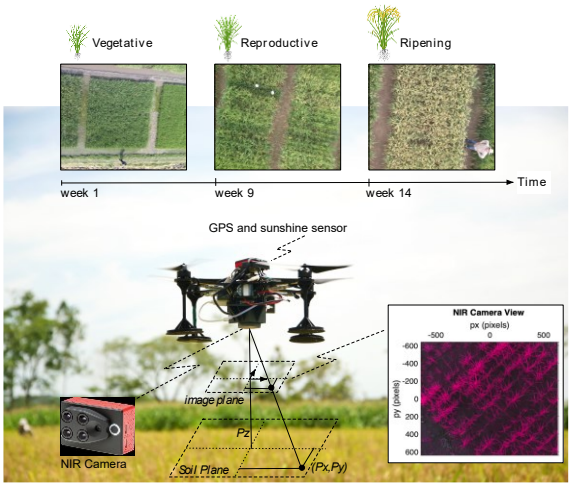

Figure 1: UAV for crop monitoring.

UAV optimization requires the modeling the effects of both UAV energy consumption and battery discharge. Here, we propose to develop a mathematical model for the optimization of the UAV energy consumption by considering the inertial dynamics, aerodynamics, and battery properties of the UAV. In [6], the development of the dynamic and aerodynamic modeling of a UAV is presented, while in [7], the modeling of the State of Charge (SoC) for the battery voltage in Li-ion batteries is presented. In [8], authors present the relationship between the SoC and the dynamic and aerodynamic model with the energy consumption of the UAV, with the aim to optimize flight efficiency. According to [8], UAVs are multi-rotor flying machines, as a consequence, a large proportion of their energy is consumed by the rotor. In [9], a DNA algorithm is used to find the lowest cost path based on the Hamiltonian. The method is twofold, since it requires the calculation of the Hamiltonian routes of the graph, to subsequently determining the lowest cost of the path.

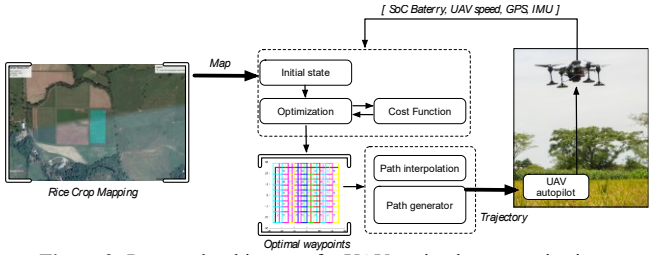

Figure 2: Proposed architecture for UAV optimal crop monitoring.

In this paper, a trajectory optimization architecture is proposed (see Fig. 2), composed by two stages: an optimal control problem supported by the dynamic optimization method of the Toolbox APMonitor with the IPOPT solver [10] [11], and the Hamiltonian algorithm that allows to find the lowest cost route for the UAV. As shown in Fig 2, the optimization model requires the area to cover, represented by a XY grid map of the crop. In this optimization problem, the altitude of the UAV is considered as constant (20m over the ground). Once the Hamiltonian is solved, the optimized set of waypoints are interpolated by using analytical functions for positions, velocities and accelerations that follow a straight-line trajectory profile.

II. Methods

The path optimization architecture is made up of four modules. The first module corresponds to the energy optimization that is carried out through an optimization model taking into account the dynamic and aerodynamic model of the UAV, thus obtaining the cost of each of the sections between the related waypoints. The second module corresponds to the route optimization through a Hamiltonian algorithm that allows finding the optimal route according to the costs calculated in the first module. On the other hand, the third module performs the trajectory planning thus generating the interpolated optimal trajectory, finally in the fourth the

978-1-6654-3331-0/20/$31.00 ©2020 IEEE

simulation of the trajectory is carried out in the Matlab Robotics Toolbox[13] (where the dynamic and aerodynamic model of the UAV and a battery model are implemented) and V-REP through an algorithm.

A. Module 1: Energy optimization

For the development of energy optimization, it is necessary to define the dynamic and aerodynamic model of the UAV. These models are defined through Newton Euler's fundamental method [6] [8], as:

$$\begin{aligned}
\ddot{x} &= \frac{(\cos(\phi)\sin(\theta)\cos(\psi)+\sin(\phi)\sin(\psi))T_b}{m} \\
\ddot{y} &= \frac{(\cos(\phi)\sin(\theta)\sin(\psi)-\sin(\phi)\cos(\psi))T_b}{m} \\
\ddot{z} &= \frac{(\cos(\phi)\cos(\theta))T_b - m\cdot g}{m} \\
\ddot{\phi} &= \frac{I_y - I_z}{I_x}\dot{\theta}\dot{\psi} + {I_x}^{-1}\tau_x \\
\ddot{\theta} &= \frac{I_y - I_z}{I_x}\dot{\phi}\dot{\psi} + {I_y}^{-1}\tau_y \\
\ddot{\psi} &= \frac{I_x - I_y}{I_z}\dot{\phi}\dot{\theta} + {I_z}^{-1}\tau_z
\end{aligned} \tag{1}$$

In (1) the dynamic model for a UAV is defined, where the navigation angles are represented by the Euler angles ϕ, θ, and ψ. The Yaw angle ψ represents the rotation around the z axis, the Picth angle θ represents the rotation around the y axis, and the Roll angle ϕ represents the rotation around the x axis, on the other hand, T_b is the total thrust generated by the rotors at the center of mass. Finally, the constants I_x, I_y and I_z are the characteristic inertias of the UAV at the center of mass, and m is the mass.

$$\begin{aligned}
\tau_x &= \overrightarrow{Scm}\,(T_4 - T_3) \\
\tau_y &= \overrightarrow{Scm}\,(T_1 - T_2) \\
\tau_z &= \overrightarrow{Scm}\,(T_3 + T_4 - T_1 - T_2)
\end{aligned} \tag{2}$$

In (2), the torques on each of the axes that are associated with the thrusts caused by the rotors T_1, T_2, T_3 and T_4 are defined. These in turn depend on the angular velocity of the rotors (ω_i), the density of the air (ρ_{air}), the Lift constant (C_L), the Drag constant (C_D) and the area of the blades (A), as shown in (3).

$$T_i = \frac{1}{2}\,\rho_{air}\,{\omega_i}^2\,A\,(C_L + C_D), \qquad i = 1,2,3,4 \tag{3}$$

Finally, the total thrust is defined as the sum of each of the thrusts generated by the rotors.

$$\begin{aligned}
T_b &= \sum_{i=1}^{4} \frac{1}{2}\,\rho_{air}\,{\omega_i}^2\,A\,(C_L + C_D) \\
T_b &= \sum_{i=1}^{4} T_i
\end{aligned} \tag{4}$$

The UAV energy model is composed of mechanical energy (kinetic and potential energy) and electrical energy. The kinetic energy depends on the inertia matrix at the center of mass and the velocity vector at the center of mass. On the other hand, the potential energy depends on the mass of the UAV, the gravity and the position with respect to the z axis.

The inertia matrix is defined, which depends exclusively on the mass of the UAV and the inertia in each axis, thus obtaining a 6x6 matrix organized as follows:

$$I_{6x6} = \begin{bmatrix} I_x & 0 & 0 & 0 & 0 & 0 \\ 0 & I_y & 0 & 0 & 0 & 0 \\ 0 & 0 & I_z & 0 & 0 & 0 \\ 0 & 0 & 0 & m & 0 & 0 \\ 0 & 0 & 0 & 0 & m & 0 \\ 0 & 0 & 0 & 0 & 0 & m \end{bmatrix} \tag{5}$$

The velocity vector at the center of mass masa V_{cm}, is defined, where ω_{cm} are the angular velocities, υ_{cm} are the translational velocities.

$$V_{cm} = [\omega_{cm} \;\; \upsilon_{cm}]^T = \left[\phi \;\; \dot{\theta} \;\; \psi \;\; \dot{x} \;\; \dot{y} \;\; \dot{z}\right]^T \tag{6}$$

The kinetic energy K is defined:

$$K = \frac{1}{2} * {V_{cm}}^T\, I\, V_{cm} \tag{7}$$

Where V_{cm} is the velocity vector at the center of mass and I the inertia matrix at the center of mass.

The potential energy P is defined:

$$P = m\,g\,z \tag{8}$$

Where m is the mass of the UAV, g is gravity, and z is the position of the UAV, so the potential energy is proportional to the position in z.

The total electrical energy consumed (E_c) is expressed as follows [8]:

$$\begin{aligned}
E_j &= \int_{t0}^{tf} \frac{(J\dot{\omega}_j(t) + k_t{\omega_j}^2(t) + D_v\omega_j(t))}{f_{r,j}(\tau_j(t),\ \omega_j(t))}\,\omega_j(t)\,dt \\
E_c &= \sum_{j=1}^{4} E_j
\end{aligned} \tag{9}$$

Where $f_{r,j}$ is the efficiency of the brushless DC motor that is defined as a function of the angular velocity and the rotor torque [8].

From the dynamic and aerodynamic model of the UAV as well as the energetic model, the following optimization model is proposed [8].

$$\min_{(\omega_j,\ \tau_j)} E_c(t_f) \tag{10}$$

Subject to

$$\begin{aligned} m\ddot{x} &= (\cos\phi\sin\theta\cos\psi + \sin\phi\sin\psi)T_b \\ m\ddot{y} &= (\cos\phi\sin\theta\sin\psi - \sin\phi\cos\psi)T_b \\ m\ddot{z} &= (\cos\phi\cos\theta)T_b - mg \\ I_x\ddot{\phi} &= (I_y - I_z)\dot{\theta}\dot{\psi} + \tau_x \\ I_y\ddot{\theta} &= (I_z - I_x)\dot{\phi}\dot{\psi} + \tau_y \\ I_z\ddot{\psi} &= (I_x - I_y)\dot{\phi}\dot{\theta} + \tau_z \end{aligned} \tag{11}$$

With the following restrictions

$$\begin{aligned} |\phi| \le \frac{\pi}{2}, \quad |\theta| \le \frac{\pi}{2}, \quad |\psi| \le \dot{\psi} \\ 0 \le \omega \le 3000 \\ 0 \le T_b \le 16 \\ |\tau_k| \le 5, \quad k = 1,2,3 \end{aligned} \tag{12}$$

Boundary conditions

$$\begin{aligned} [x(t_0), y(t_0), z(t_0), \phi(t_0), \theta(t_0), \psi(t_0)]^T &= [x_0, y_0, z_0, 0, 0, 0]^T \\ [x(t_f), y(t_f), z(t_f), \phi(t_f), \theta(t_f), \psi(t_f)]^T &= [x_f, y_f, z_f, 0, 0, 0]^T \\ [\dot{x}(t_f), \dot{y}(t_f), \dot{z}(t_f), \dot{\phi}(t_f), \dot{\theta}(t_f), \dot{\psi}(t_f)]^T &= [0, 0, 0, 0, 0, 0]^T \\ \omega_j(t_0) = 912.32\ rad/s, \quad j &= 1,2,3,4 \end{aligned} \tag{13}$$

In (10) minimization of the objective function is presented, in (11) the intrinsic restrictions of the problem are presented that are due to the nature of the UAV, in (12) the limits of the navigation angles are presented that allow navigation without aggressive maneuvers that can destabilize the UAV, as well as other restrictions that help the algorithm to converge towards an optimal solution, and in (13) the initial and final conditions of the UAV are presented in such a way that the east starts from rest at a point initial (x_0, y_0, z_0) until reaching the end point (x_f, y_f, z_f) where again the linear and angular velocities return to zero.

Note that the initial condition of the engine speed is set at $912.32\ rad/s$, so the total thrust is $T = 12.75\ N$, which corresponds to the thrust necessary to counteract the action of gravity, and that the UAV floats from balanced form.

Finally, iterating the start and end positions according to the relationships between the waypoints, the cost between each leg of the related waypoints is found.

$$costs = \begin{bmatrix} waypoint_i & cost_1 & waypoint_f \\ \vdots & \ddots & \vdots \\ waypoint_{in} & cost_n & waypoint_{fn} \end{bmatrix} \tag{14}$$

B. Module 2: Route Optimization

From the route costs obtained in module 1, the route optimization is developed through a Hamiltonian algorithm [9].

The waypoints system is modeled using directional graphs and representing the energy consumption between waypoints through the edges of the graph. Then, the different routes that the UAV can follow are generated from permutations, and the combinations that can be carried out through the graph according to its direction of movement are searched.

Finally, from the possible combinations, the route with the minimum cost is found, this being the route with the least energy consumed.

C. Module 3: Trajectory Planner

To generate a line segment in cartesian space, one can start from the equation of the line in Cartesian space in order to express each of the coordinates through the parametric equations of the line [12].

$$f(x, y, z) = \lambda(t)(p_1 - p_0) + p_0 \tag{15}$$

Where x, y and z represent the Cartesian coordinates in space, t represents the sampling time that allows controlling the speed of the line, p_0 and p_1 represent the initial and final points of the line respectively [12]. The trapezoidal velocity profile is shown in Figure 1.

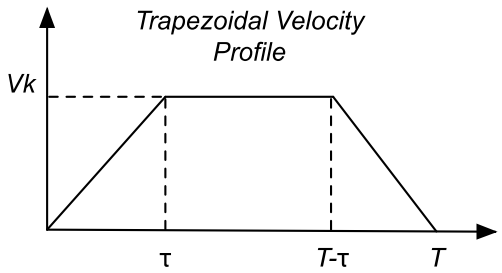

Figure 1: Trapezoidal velocity profile [12].

The trapezoidal velocity profile is made up of three sections, these are the acceleration, constant speed and deceleration section, where τ represents the acceleration time and T represents the total travel time. The first leg and third leg are uniformly accelerated movements (MUA), and the second leg is a constant velocity movement.

The section of acceleration begins at $P(0)$ where it starts from rest and ends at $P(\tau)$ where it reaches the maximum velocity of the trajectory. Then, from point $P(\tau)$, the constant speed section begins, with the maximum speed acquired in the first section remaining up to point $P(T-\tau)$. Finally, from point $P(T-\tau)$, the deceleration stretch begins until returning to rest at point $P(T)$.

The trapezoidal velocity profile is described in the following piecewise function [12]:

$$f(t) = \begin{cases} f_a, & 0 \le t \le \tau \\ f_v, & \tau \le t \le T - \tau \\ f_d, & T - \tau \le t \le T \end{cases} \quad (16)$$

Where f_a is the acceleration section, f_v is the constant velocity section and f_d is the deceleration section.

The acceleration section f_a is defined:

$$f_a = \frac{1}{|P(\tau) - P(0)|}\left(\frac{1}{2}at^2\right)\big(P(\tau) - P(0)\big) + P(0) \quad (17)$$

The constant velocity section f_v is defined:

$$f_v = \frac{V_k \cdot t}{|P(T-\tau) - P(\tau)|}\big(P(T-\tau) - P(\tau)\big) + P(\tau) \quad (18)$$

The deceleration section f_d is defined:

$$f_d = \frac{1}{|P(T) - P(T-\tau)|}\left(\frac{1}{2}at^2 + V_k \cdot t\right)\big(P(T) - P(T-\tau)\big) + P(T-\tau) \quad (19)$$

Finally, through this module the interpolated optimal route is generated.

D. Module 4: Trajectory simulation

For the simulation of the trajectory, the Matlab Robotics Toolbox [13] was used, where the Li-ion battery model and the energy model were incorporated to monitor the operation of the developed algorithms.

In order to have a simulation environment closer to real life, the V-REP software is linked with the optimization architecture designed in Matlab. In the V-REP software, a simulation environment is created through the different figures offered by the software and in addition to the textures and 3D elements obtained on the web.

Figure 2: Simulation environment in V-REP.

The Figure 2 presents the simulation environment designed, which has ten plots distributed in the crop.

III. Results and Discussion

Three tests are carried out to verify the complete operation of the path optimization algorithm. Then, from the results, the simulation of each trajectory is carried out using the Matlab Robotics Toolbox on which the energy and battery model was implemented.

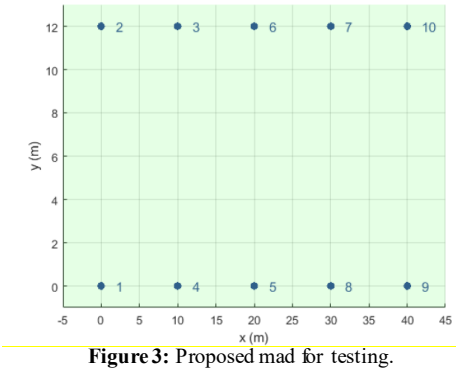

Figure 3: Proposed mad for testing.

In order to have a clearer picture of the operation of the algorithm, the simulation of three non-optimal trajectories is carried out, so that there is a simulation with the optimal trajectory designed by the algorithm, which delivered the same trajectory in the three tests and a simulation of a non-optimal trajectory with the same parameters and initial conditions for each of the tests, as can be seen in figure 4 and figure 5.

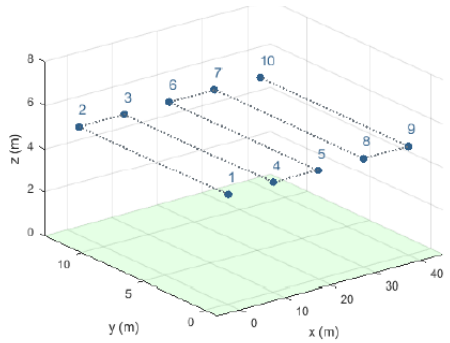

Figure 4: Not optimal trajectory.

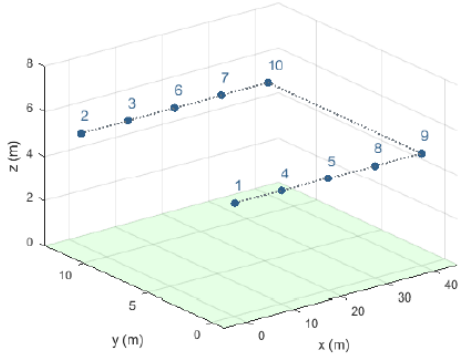

Figure 5: Optimal trajectory.

978-1-6654-3331-0/20/$31.00 ©2020 IEEE

A. Test 1: Fully charged battery

In test 1, the trajectory optimization is performed on the map presented in figure 3, with the UAV battery fully charged, and under a maximum speed of 1 m/s. **Table 2** presents the initial conditions used for the simulations of both the optimal path and the non-optimal path.

Parameter	Value
Maximum Speed (V_k)	$1m/s$
Percentaje of aceleration (pt)	30%
Sampling time (tm)	$0.166ms$
Initial Position	$x = 0 \;\; y = 0 \;\; z = 5$
Height	$5m$
Initial battery voltage	$11V$
Initial battery status (SoC)	100%

Table 2: Parameters and initial conditions test 1.

Through the simulations carried out, the following results are obtained:

Type of energy	Not optimal trajectory	Optimal Trajectory
Mission Time	$142.8271s$	$131.4286s$
Battery Status (SoC)	45%	57%
Kinetic Energy	$5568.3kJ$	$4806.14kJ$
Potential Energy	$3.17mJ$	$3.14mJ$
Electric energy (consumed by engines)	$66.32kJ$	$61.9kJ$
Total Energy	$5634.62kJ$	$4868.04kJ$

Table 3: Results of test 1.

In table 3 it can be seen that each type of energy (kinetic, potential and electrical) decreases in the optimal path with respect to the simulated non-optimal path. Table 4 shows the optimization percentage for each type of energy.

Type of energy	Percentage of optimization
Kinetic Energy	13.7%
Potential Energy	1%
Electric Energy (consumed by engines)	6.7%
Total Energy	13.6%

Table 4: Optimization percentages of test 1.

Through the results shown in table 3 and table 4, the operation of the optimal navigation architecture designed is corroborated, which allows reducing the total energy consumed by 13.6%.

B. Test 2: Battery with critical state of charge

In test 2 the trajectory optimization is carried out on the map presented in figure 3, with the UAV battery charged to 44% which implies a critical state of charge for the simulated non-optimal trajectory, and under a maximum speed of $1\ m/s$. Table 5 presents the initial conditions used for the simulations.

Parameter	Value
Maximum speed (V_k)	$1m/s$
Percentage of acceleration (pt)	30%
Sampling time (tm)	$0.166ms$
Initial Position	$x = 0 \;\; y = 0 \;\; z = 5$
Height	$5m$
Initial battery voltage	$9.873V$
Initial battery status (SoC)	44%

Table 5: Parameters and initial conditions test 2.

Through the simulations carried out, the following results are obtained:

Type of energy	Not optimal trajectory	Optimal Trajectory
Mission Time	$142.8271s$	$131.4286s$
Battery Status (SoC)	45%	57%
Kinetic Energy	$5568.3kJ$	$4806.14kJ$
Potential Energy	$3.17mJ$	$3.14mJ$
Electric energy (consumed by engines)	$66.32kJ$	$61.9kJ$
Total Energy	$5634.62kJ$	$4868.04kJ$

Table 6: Results of test 2.

In table 6 it can be seen that each type of energy (kinetic, potential and electric) decreases in the optimal path with respect to the simulated non-optimal path. In addition, according to the results obtained in the simulations, it can be corroborated that the UAV covers more area with a low battery thanks to the designed optimization algorithm. It can also be seen that the optimal trajectory obtained through the algorithm requires less time to complete the journey with respect to a non-optimal trajectory. Table 7 shows the percentage of optimization for each type of energy.

Type of energy	Percentage of optimization
Kinetic Energy	13.7%
Potential Energy	1%
Electric Energy (consumed by engines)	6.7%
Total Energy	13.6%

Table 7: Optimization percentages of test 2.

Through the results shown in table 6 and table 7, the operation of the optimal navigation architecture designed is corroborated, which allows reducing the total energy consumed by 13.6%.

C. Test 3: Trajectory with maximum speed of 2 m/s

In test 3 the trajectory optimization is performed on the map presented in figure 3, with the UAV battery fully charged, and under a maximum speed of 2 m/s. Table 8 presents the initial conditions used for the simulations.

Parameter	Value
Maximum speed (V_k)	$2m/s$
Percentage of acceleration (pt)	30%
Sampling time (tm)	$0.166ms$
Initial Position	$x = 0 \quad y = 0 \quad z = 5$
Height	$5m$
Initial battery voltage	$11V$
Initial battery status (SoC)	100%

Table 8: Parameters and initial conditions test 3.

Through the simulations carried out, the following results are obtained:

Type of energy	Not optimal trajectory	Optimal Trajectory
Mission Time	$71.4286s$	$65.5s$
Battery Status (SoC)	86%	88%
Kinetic Energy	$1412.52kJ$	$1220.22kJ$
Potential Energy	$4.23mJ$	$3.94mJ$
Electric energy (consumed by engines)	$34.81kJ$	$32.45kJ$
Total Energy	$1447.3kJ$	$1252.67kJ$

Table 9: Results of test 3.

In table 9 it can be seen that each type of energy (kinetic, potential and electric) decreases in the optimal path with respect to the simulated non-optimal path. Table 10 shows the percentage of optimization for each type of energy.

Typo of energy	Percentage of optimization
Kinetic Energy	13.6%
Potential Energy	6.8%
Electric Energy (consumed by engines)	6.7%
Total Energy	13.4%

Table 10: Optimization percentages of test 3.

Through the results shown in table 9 and table 10, it can be seen that the total energy consumed decreases by 13.4% for test 3.

IV. Conclusions

The development of the energy optimization algorithm which has the Newton-Euler dynamic model as restrictions and was implemented in the MATLAB software through the IPOPT solver, is solved with great ease and flexibility to the change of parameters or initial and final conditions, which It provides a wide range of changes that is proportional to the range of tests that you want to implement. It can also be observed that due to the robustness of the model, it could require a certain waiting time to obtain the optimal response. It is recommended for similar implementations to have previous knowledge of dynamic optimization and an intermediate level of familiarity with the IPOPT solver.

The optimization percentage depends on each map and the number of waypoints on it, so a larger map, as well as a larger number of waypoints, would allow a higher optimization percentage.

The optimization implemented to different processes, in this case specifically to agriculture, is extremely important since it allows a task to be carried out in the most efficient way, in the best of cases, using the least amount of resources which translates into less effort and more importantly at lower costs. This development focused on this field allows the constant study of crops for the realization of strategies with the objective of developing models for the improvement of food security and environmental sustainability of agricultural systems.

In the future, a multi-objective optimization could be implemented in which, in addition to minimizing the energy consumed in the trajectory, the mission time is minimized, in order to obtain greater efficiency in the designed trajectories.

Acknowledgments

This work was funded by the OMICAS program: Optimización Multiescala In-silico de Cultivos Agrícolas Sostenibles (Infraestructura y validación en Arroz y Caña de Azúcar), anchored at the Pontificia Universidad Javeriana in Cali and funded within the Colombian Scientific Ecosystem by The World Bank, the Colombian Ministry of Science, Technology and Innovation, the Colombian Ministry of Education and the Colombian Ministry of Industry and Turism, and ICETEX under GRANT ID: FP44842-217-2018 and OMICAS Award ID: 792-61187.

V. References

[1] https://www.omicas.co/que-es-omicas

[2] http://www.asctec.de/downloads/public/HB_AscTec-Hummingbird_safety-data-sheet.pdf.

[3] https://www.bhphotovideo.com/lit_files/259641.pdf.

[4] https://dl.djicdn.com/downloads/Mavic%20Air/Mavic%20Air%20User%20Manual%20v1.0.pdf.

[5] www.dji.com

[6] Towards Miniatura MAV Autonomous Fligth: A Modeling & Control Approach, Julian D. Colorado M., abril 2009.

[7] Li-ion Battery Emulator for Electric Vehicle Applications, T. Meshabi, N. Rizoug, P. Bartholomeüs y P. Le Moigne, octubre 2013.

[8] Optimization of Energy Consumption for Quadrotor UAV, Yacef Fouad, Omar Bouhali, Nassim Rizoug y Mustapha Hamerlain, septiembre 2017.

[9] Solving Shortest Hamiltonion Path Problem Using DNA Computing, H. Mohammed Alshamlan y M. El Bachir Menai, 2012.

[10] Nonlinear Modeling, Estimation and Predictive Control in APMonitor, Hedengren, J. D. and Asgharzadeh Shishavan, R., Powell, K.M., and Edgar, Computers and Chemical Engineering, Volume 70, pg. 133–148, 2014, doi: 10.1016/j.compchemeng.2014.04.013.

[11] GEKKO Optimization Suite, Beal, L.D.R., Hill, D., Martin, R.A., and Hedengren, J. D., Processes, Volume 6, Number 8, 2018, doi: 10.3390/pr6080106.

[12] Planeación de trayectorias, Diapositivas de la clase Herramientas para Robótica, Julian D. Colorado M., Pontificia Universidad Javeriana.

[13] https://petercorke.com/toolboxes/robotics-toolbox/.